ESTIMATE OF THE DOMAIN ORIENTATION DISTRIBUTION FUNCTION AND THE THERMOELASTIC PROPERTIES OF PYROLYTIC CARBON BASED ON A IMAGE PROCESSING TECHNIQUE

T. Böhlke*, S. Lin*, T.-A. Langhoff*, R. Piat*,
Institute of Engineering Mechanics, Department of Mechanical Engineering,
Karlsruhe Institute of Technology, Germany
* {boehlke, lin, langhoff, piat}@itm.uni-karlsruhe.de

1 Introduction

Pyrolytic carbon (PyC) is a graphite-like material with complex multiscale microstructure that can be used under severe thermal loadings. By using experimental characterization methods like high-resolution transmission electron microscopy (HRTEM) with selected-area electron diffraction [1] the microstructure of PyC can be described as a set of coherent domains having different orientations. The aim of this work is basing on the real microstructure to identify the parameter of the domain orientation distribution function (DODF). On the spot of DODF the orientations of all domains are reconstructed and applied to homogenize the thermoelastic properties of PyC [4]. Due to automatically extract these domains in HRTEM images, texture segmentation is employed.

2 Image Processing

2.1 Texture Segmentation

Generally, segmentation refers to the process of partitioning a digital image into multiple segments (sets of pixels). The goal of segmentation is to simplify and/or change the representation of an image for an easier and more meaningful analysis. In order to reliably distinguish between two domains, representative features must be available. An efficient method for image segmentation based on texture description with feature distributions is the so-called Local Binary Patterns (LBP) method [2]. The approach of the LBP operator works generally with eight neighbors of a pixel, using the value of the center pixel as a threshold. An LBP code for a neighbor is produced by multiplying the thresholded values with weights given to the corresponding pixels, and summing up the result. The texture segmentation algorithm based on LBP operator consists of three steps: hierarchical splitting, agglomerative merging and pixelwise classification. An example of segmentation result is shown in Figure 1 [3].

After the segmentation, Fourier-analysis can be used to gain the distribution of the angle α and layer spacing *d* [3]. Note that the spacing *d* is not considered in this work, because of accurate undeterminability of the layer spacing *d* on the submicron level by imaging of HRTEM. The precise measurement depends on a preferred preparation of material specimen.

2.2 Global Analysis

Laplacian filters are applied on a smoothed image (e.g., using a Gaussian filter). This two-step process is so-called Laplace of Gaussian (LoG) operation. The LoG operator takes the second derivative of the image. Where the image is basically uniform, the LoG will give zero. Wherever a change of grey values occurs, the LoG will give a positive response on the darker side and a negative response on the lighter side. After Gaussian smooth the performance of Fourier Transformation (FT) is improved obviously (See Fig. 7). Aim to minimize information lost the window size of LoG filter is chosen as 5×5 and $\sigma = 0.5$.

With the specific preprocessing of a LoG filter on a TEM image the global FT gains the estimate of distribution function of the microstructures. Locally, every domain with homogeneous texture is extracted by using texture segmentation method. Both results

indicate the domain orientation distribution function of the microstructure can be modeled by von Mises-Fisher distribution.

3 Domain Orientation Distribution Function and Homogenization

3.1 von Mises-Fisher Distribution

For simplicity we model the orientation distribution of domains based on a one-parameter axial orientation distribution function. We can use Fisher distributions for modeling the orientation of the unit normal vectors of the graphene planes [4]. That depends on the so-called concentration parameter κ .

As shown in Fig. 2 if we consider a single fiber with carbon deposited on it, we define our coordinate system to have the $\mathbf{e}_3$-axis parallel to the fiber-axis. In Fig. 3 the mean direction of the $\bar{\mathbf{c}}$-axis can be interpreted as the mean growth direction of the graphene domains. It is set up as follows depending on the angle γ:

$$\bar{\mathbf{c}}(\gamma) = \cos(\gamma)\mathbf{e}_1 + \sin(\gamma)\mathbf{e}_2, \qquad \gamma \in [0, \pi].$$

By using the angle α and taking into account the angle γ we obtain the probability density $f_\alpha(\alpha, \gamma)$ based on the von-Mises-Fisher distributions in the following analytical form

$$f_\kappa(\alpha, \gamma) = \frac{1}{4\pi} \int_0^{\pi/2} \frac{\kappa}{\sinh(\kappa)} \cosh(\kappa \sin(\upsilon)\cos(\varphi - \gamma)) \sin(\upsilon) \mathrm{d}\upsilon,$$

where the angle $\alpha \in [0, \pi]$ is provided by the aforementioned texture segmentation; Alternatively, the integration in above equation can be rewritten by modified Struve function $L_{-1}(.)$ [5],

$$f_\kappa(\alpha, \gamma) = \frac{\kappa}{4\sinh(\kappa)} L_{-1}(\kappa \sin(\gamma - \alpha)),$$

that can be represented as power series. In Fig. 4 the probability density functions f_κ are plotted with different κ using $\gamma = \pi/2$, i.e., $\bar{\mathbf{c}} = \mathbf{e}_2$. The results indicate that if $\kappa \to 0$, the DODF distributes uniformly, in a contrary manner, if $\kappa \to \infty$, the DODF is much sharper and approaches orientation of only one domain.

3.2 Estimate of Parameters

Based on the texture segmentation results the concentration parameter κ and the angle γ can be statistically estimated by Maximum-Likelihood-method [6]. The 2D plots of log-likelihood functions depending on κ and γ are represented in Fig. 5. As shown in the plots we find the unique local maximum of the log-likelihood functions, and then the best fitted concentration parameter and the orientation of $\bar{\mathbf{c}}$ of the specific HRTEM images (see Fig. 1(a)) can be estimated.

3.3 Elastic and Thermoelastic properties

The effective elastic properties of pyrolytic carbon on the submicron scale can be homogenized using Fisher distributions [4]. With the estimated κ the homogenization results are represented in Fig. 6. The 1st-order bounds (Voigt & Reuss bounds) and 2nd-order bounds (Hashin-Shtrikman (HS) upper & lower bounds) of thermoelastic properties of PyC can be given taking into account functional variation of free energy analogically. An example results of thermal stress tensor β (top: HS upper bounds; down: HS lower bounds) are presented as follows:

$$\beta^{\text{HS upper}} = \begin{pmatrix} 14.78 & -0.004 & -0.04 \\ & 14.79 & 0.035 \\ \text{Sym.} & & 23.6 \end{pmatrix}$$

$$\beta^{\text{HS lower}} = \begin{pmatrix} 4.23 & -0.003 & -0.05 \\ & 4.24 & 0.042 \\ \text{Sym.} & & 14.95 \end{pmatrix}$$

4 Conclusions and Perspectives

In this work the DODF is modeled by von Mises-Fisher distribution based on the real microstructure of PyC. Simultaneously, the LBP segmentation algorithm and the Fourier analysis are set up to understand the characteristics of microstructure in HRTEM images. Due to estimate the parameters of the probability density function, Maximum-Likelihood-Method is archived on the spot of the results of image processing techniques. After that the effective thermoelastic properties of PyC, e.g., HS upper and lower bounds, are homogenized with variation theory.

In further work other numerical methods gathering the necessary data set will be compared with the texture segmentation. Furthermore, HRTEM image is only one of the possibilities to observe the microstructure of carbon materials, the source information can be given by other experimental techniques, surely, and these challenge the issue into higher dimensional spaces.

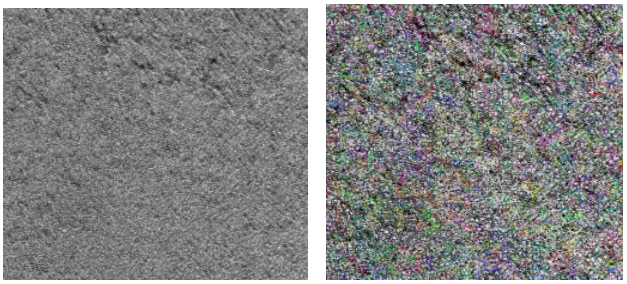

(a) (b)

Figure 1: (a) TEM image size: 1000×1000 [pixel] and scale: 0.05 [nm/pixel]; (b) Segmentation result of (a) [3].

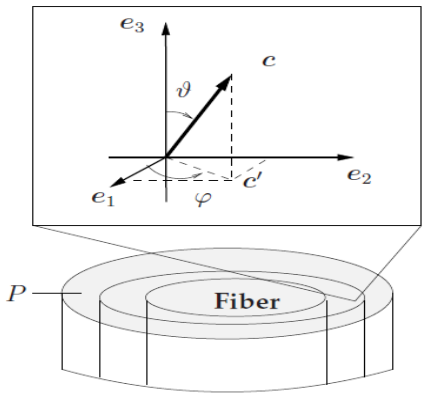

Figure 2: Cross-section plane P of Fiber.

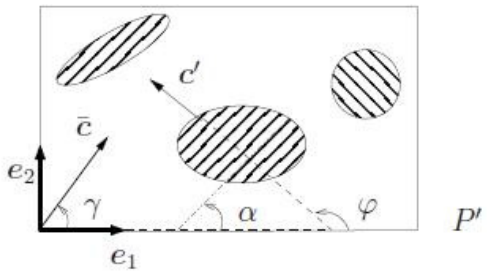

Figure 3: Image plane P'.

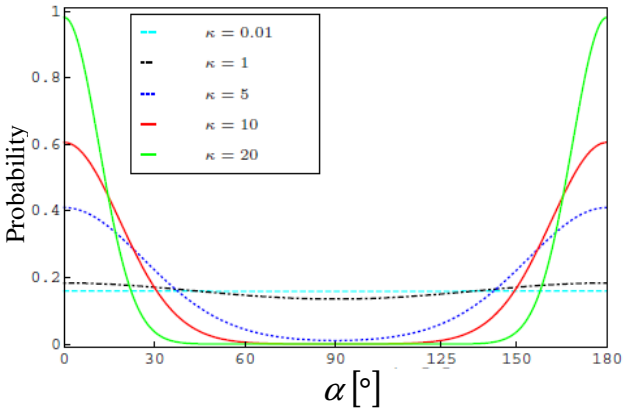

Fig. 4: Illustration of probability density function referring to the angle α.

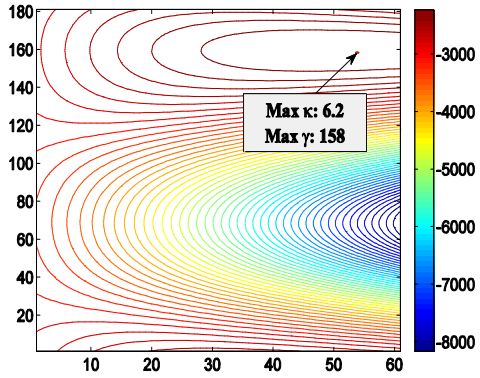

Fig. 5: 2D plot of log-likelihood function of HRTEM image in Fig. 1(a).

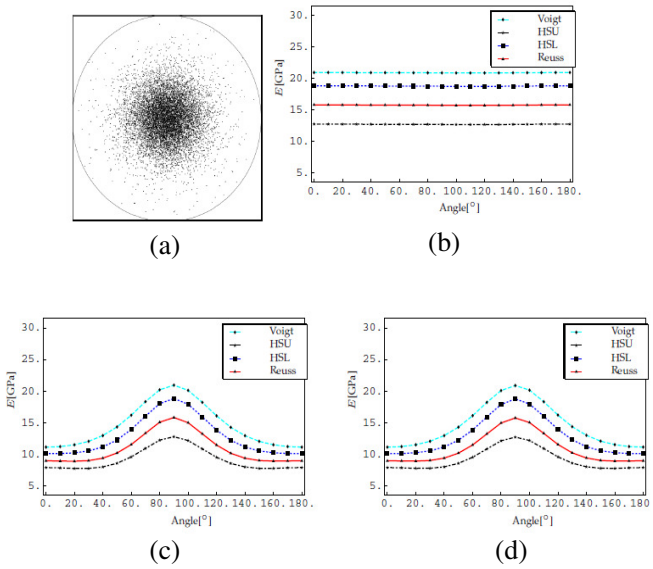

Fig. 6: (a) Pole figure; (b) Young's modulus in principal plane $\mathbf{e}_1 - \mathbf{e}_2$; (c) Young's modulus in principal plane $\mathbf{e}_1 - \mathbf{e}_3$; (d) Young's modulus in principal plane $\mathbf{e}_2 - \mathbf{e}_3$.

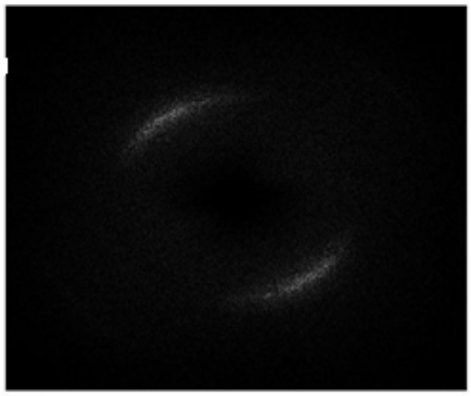

Fig. 7: FT + LoG filter result of Fig. 1(a).

Acknowledgments. The authors gratefully acknowledge support by the DFG-NSF joint grant within the "Materials World Network: Multi-scale study of chemical vapor infiltrated C/C composites".

References

[1] B. Reznik, D. Gerthsen, W. Zhang, K. Hüttinger, "Texture changes in the matrix of an infiltrated in a carbon fiber felt studied by polarized light microscopy and selected area electron diffraction". *Carbon*, 41(2), 376-380, 2003.

[2] T. Ojala, M. Pietikäinen, "Unsupervised texture segmentation using feature distributions". *Pattern Recognition*, 32(3), 477-486, 1999.

[3] T. Böhlke, S. Lin, R. Piat, M. Heizmann , I. Tsukrov, "Estimate of the Thermoelastic Properties of Pyrolytic Carbon based on an Image Segmentation Technique". *PAMM*, 10: 281–282

[4] T. Böhlke, K. Jöchen, R. Piat, T.-A. Langhoff , I. Tsukrov, B. Reznik, "Elastic properties of pyrolytic carbon with axisymmetric textures". *Technische Mechanik*, 30(4), 343-353, 2010.

[5] M. Abramowitz, I: A. Stegun, "Handbook of mathematical functions with formulas, graphs and mathematical tables". *New York: Dover*, 498, 1998.

[6] D. Basu, "Statistical information and likelihood". *Springer-Verlag*, 45, 1988.